Original scientific paper

RESEARCH ON THE FLUID-INDUCED EXCITATION CHARACTERISTICS OF THE CENTRIFUGAL PUMP CONSIDERING THE COMPOUND WHIRL EFFECT

Wenjie Zhou[1], Dongliang Yu[1], Yifan Wang[1], Junlin Shi[2], Bin Gan[2]

[1]School of Energy and Power Engineering, Jiangsu University, Zhenjiang, China
[2]School of Mechanical Engineering, Sichuan University of Science & Engineering, Zigong, China

Abstract. *In order to study the correlation mechanism between the flow characteristics and the fluid-induced force under the compound whirl motion in the centrifugal pump, the RNG k-ε model is selected in this paper to simulate a low specific speed centrifugal pump with impeller eccentricity based on the N-S equation. The changes of fluid-induced force with impeller eccentricity and the unsteady flow characteristics of the internal flow field of centrifugal pump under different flow conditions and rotation speeds are investigated, and the relationship between the fluid-induced force of the impeller and the internal flow field characteristics is discussed. The results show that the trend of fluid-induced force and the pressure coefficient is similar. When the rotation speed changes and when the flow is similar, the pressure coefficient under different rotation speeds almost coincides. With the increase of impeller speed and impeller eccentricity, the dynamic and static interferences between the impeller and the volute tongue are more significant, the uneven distribution of the pressure around the impeller makes the internal flow of centrifugal pump more disordered and increases the fluid-induced force near the volute tongue. The research results can provide important reference value for accurately grasping the internal flow excitation principle of the centrifugal pump.*

Key Words: *Centrifugal Pump, Compound Whirl, Fluid-induced Force, Internal Flow Characteristics*

1. INTRODUCTION

Centrifugal pumps are widely used in many fields, such as water supply, irrigation and liquid transportation, etc. As one of the investigation focuses, the internal flow phenomena and the characteristics have been given much attention because the flow in the pump is

complicated and unordered [1-6]. There are many factors affecting the flow characteristics of the centrifugal pump, among which, the wake flow of blade and the dynamic and static interference between the impeller and the volute tongue are the two key factors [7, 8]. Actually, due to various assembly errors in centrifugal pumps, the geometric center of the impeller does not coincide with the mass center [9]. This phenomenon could generate fluid excitation force and change the dynamic characteristics of the rotor system. Therefore, it is important to study the inner flow characteristics and corresponding fluid-induced force of the centrifugal pump considering the eccentric whirl motion of the impeller.

The inner flow characteristics are helpful to reveal the essence of fluid-induced vibration of the centrifugal pump. Liu et al. [10] analyzed the pressure fluctuations by CFD tool and found that the three-dimensional inlet guide vane can reduce the amplitude of the impeller pressure fluctuation at a small flow rate and a design flow rate. Bai et al. [11] proposed a smaller number of diffuser blades, which could reduce the pressure fluctuation in the diffuser. Zhang et al. [12] found that changing the shape of the blade trailing edge could greatly improve the flow field at the outlet of the blade and reduce the pressure fluctuation in the centrifugal pump. Yang et al. [13] believed that the time series effect had a great influence on the rotor-stator interaction (RSI) and the change of the inducer blade position could reduce the pressure fluctuation. Tao et al. [14] pointed out that increasing the flow area of the volute could reduce the pressure fluctuation in the volute and the radial force imposed on the shaft. Chalghoum et al. [15-17] studied the influence of static and dynamic interference between the impeller and the volute tongue on internal flow and fluid excitation effect. Zou et al. [18] explored the flow field around the impeller and transient fluid excitation effect during the start-up for a large double suction centrifugal pump. Tao et al. [19] studied the pressure fluctuation of the impeller by the separated eddy numerical simulation method and pointed out that the predicted value of the pressure fluctuation could not be in good agreement with the experimental value without considering the eccentricity of the impeller. In addition, the influence of clearance on the flow field and fluid excitation effect in pumps is also studied [20-22]. Actually, the numerical simulation has become an effective research method for different scale flow problems in engineering [23, 24].

Fluid-induced force is another manifestation of fluid excitation effect, which plays a vital impact on the vibration and stability of centrifugal pumps. Yao et al. [25] found that the displacement degree of the centrifugal pump shaft increased obviously with the decrease of the flow rate. During the start-up of the centrifugal pump, the direction of radial force acting on the pump shaft is the same as the displacement direction of the pump shaft under the condition of a small flow rate. Tan et al. [26] pointed out that the interaction between the rotor and the stator had a great influence on the fluid-induced force, but the rotation speed had a limited influence on it. Li et al. [27] changed the load distribution of the blade and found that the front-loaded impeller made the flow inside the pump more uniform, which could reduce the fluid-induced force. Barrio et al. [28, 29] obtained the unsteady pressure distribution through the pressure sensor and radial integration of the pressure on the clearance side. The results showed that the numerical results of the fluid-induced force were in good agreement with the experimental results. Karaskiewicz et al. [30] examined the correlation between the fluid-induced force and the axial thrust moment of the centrifugal pump. Zhou et al. [31] studied the influence of different flow rates, eccentricities and whirl ratios on the flow induced force of the impeller. It is found that the flow induced force is closer to the experimental data when considering the

eccentricity of the impeller, and the fitting model of the flow induced force is established. Alemi et al. [32] explored the influence of multi-volute structure on hydraulic performance and the impeller fluid-induced force under off-design conditions. Jiang et al. [33] found that the fluid-induced force of the impeller would become larger when the diffuser blade approached the volute tongue while the pressure fluctuation intensity and efficiency were reduced. It is suggested that the volute should be placed between the two blades to improve the performance of the centrifugal pump. Besides, the effects of the fluid-induced force on the pump rotor system also attracted more and more researchers with the development of different fluid excitation models in recent years [34-39].

Even the fluid-induced force of the impeller has drawn a lot of attention; most of the studies only consider the self-rotation and ignore the impeller's whirl motion. In fact, the real work condition of the impeller includes not only self-rotation but also the orbit motion whirling around the geometric center of the impeller due to eccentricity. The compound motion plays a vital influence on the fluid-induced vibration characteristics of the centrifugal pump. Besides, the relationship between the internal flow structures and the macroscopic fluid exciting force still needs further investigation. Therefore, a novel model of the centrifugal pump including the compound motion is proposed in order to explore the fluid excitation characteristics in this paper. In order to verify the accuracy of calculation model, the performance curves of numerical simulation and experimental test are compared. The changing trends of the impeller fluid-induced force under different eccentricities, flow rates and rotational speeds are studied respectively. Based on the results, the distribution law of the impeller fluid-induced force is researched and the correlation mechanism between the unsteady flow characteristics and the impeller fluid-induced force is also discussed. The results are helpful to enrich the impeller model of the centrifugal pump and provide an important reference for further coupled vibration of the rotor system.

2. 3-D MODEL OF CENTRIFUGAL PUMP

The research object is a low specific speed centrifugal pump with cylindrical blades. The three-dimensional model of this centrifugal pump mainly includes five parts: inlet, impeller, clearance, volute and outlet. The impeller offsets along the outlet direction with different eccentricities for whirl motion. The corresponding design parameters and assembled 3-D calculation model can be seen in Table 1 and Fig. 1, respectively. H_d is the head, Q_d is the flow rate, Z is the blade number, Ω is the rotation speed, n_s is the specific speed, D_1 is the inlet/outlet diameter, D_2 the impeller outlet diameter, D_3 is the volute inlet diameter.

Table 1 Main design parameters of centrifugal pump

Parameters	H_d(m)	Q_d(m^3/h)	Z	Ω(r/min)	n_s	D_1(mm)	D_2(mm)	D_3(mm)
Value	20	55	6	1450	69	80	260	290
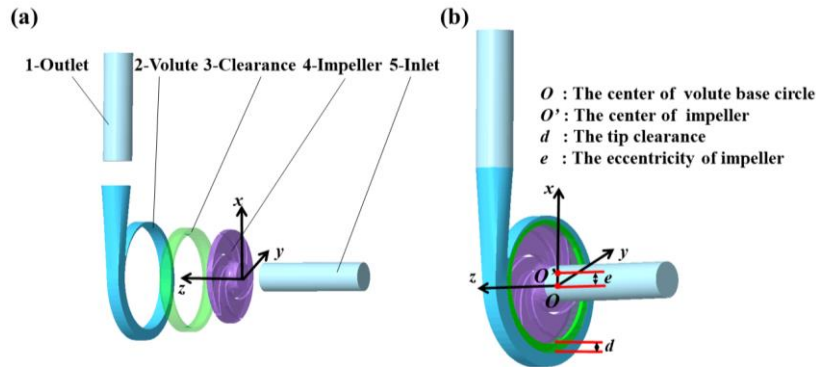
Fig. 1 3-D model of centrifugal pump (a) explosion form and (b) assembly form

The impeller rotates around its own rotating center at rotation speed Ω; meanwhile it rotates around the center of the volute base circle at whirl speed ω in the same circumferential direction. These two different motions construct the actual motion of the centrifugal pump impeller.
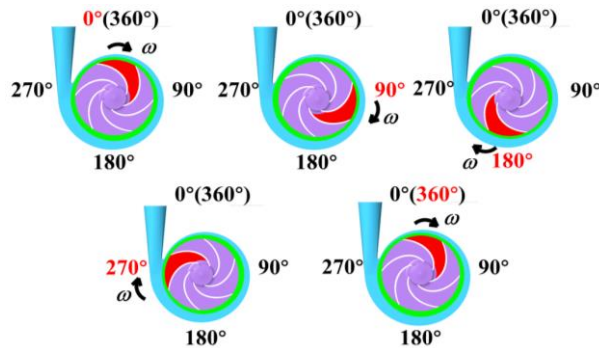
Fig. 2 Precession motion of the centrifugal pump impeller

The distance between above two centers is e, which is the impeller eccentricity, ε is the eccentricity ratio of e to the initial clearance width d of the impeller. The precession motion of the centrifugal pump impeller in a period is shown in the Fig. 2.

3. NUMERICAL CALCULATION METHOD

Based on the N-S equation, the RNG k-ε model is selected to flow analysis because it has higher calculation accuracy for a high strain rate flow and complex flow in the centrifugal pump [40]. The impeller and clearance domains are set as rotating domains, the volute, inlet and outlet domains are kept as static reference frame, the interface between static and rotating domains is applied to exchange flow field data. The boundary of inlet and outlet is set as velocity inlet and free outflow, respectively, to describe the actual flow condition. Besides, the wall is set as sliding boundary and standard wall function. The time

step in unsteady calculation is set to $\Delta t = 1.1494 \cdot 10^{-4}$ s to ensure the Coulomb number is less than 1.

In addition, the prediction head is taken as the criterion of grid independence to ensure the accuracy of calculated results before the unsteady flow research. The grids in each domain are divided and merged, and the design conditions with different grids are calculated. When the difference between each two predictions is less than 0.5%, the smaller grid is considered as the best grid because it has high accuracy and can save computing resources [41].

4. VERIFICATION OF THE COMPUTATIONAL MODEL

In order to verify the accuracy of the proposed model, the head and efficiency curves under two different conditions of non-eccentricity and 3%-eccentricity are calculated, respectively. The comparison results between the simulation and experiment [42] from $0.8Q_d$ to $1.2Q_d$ are shown in Fig. 3.

It is seen that the minimum error between the simulated head and experimental head when $\varepsilon = 0.03$ is 0.32% at design flow while the maximum error is 0.75% at $0.8Q_d$. The minimum and maximum errors without considering the whirl motion are 1.10% and 2.29%, respectively. Besides, the comparison for pump efficiency presents the similar results. When eccentricity is considered, the minimum and maximum errors are 0.05% and 0.60%, respectively. While they change to 0.59% and 1.75%, respectively, the self-rotation motion is only considered. The verification implies that the flow analysis considering the compound whirl effect of the impeller has a better calculation accuracy compared with the present self-rotation model. This is because the proposed model is closer to the actual motion status of the centrifugal pump impeller and it can better predict the inner flow characteristics.
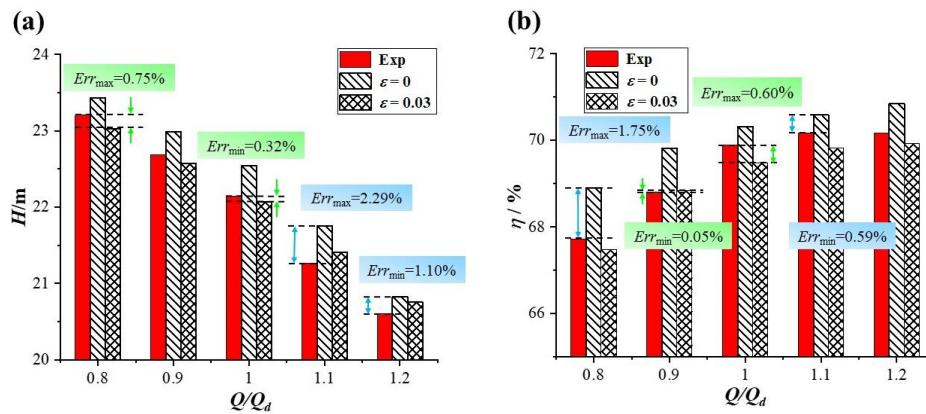
Fig. 3 Comparison of the experimental and simulated results (a) head and (b) efficiency

5. COMPUTATIONAL RESULTS AND ANALYSIS

5.1. Effects of ε, Q and Ω on F_r and C_{pRMSE}

The fluid-induced force of the impeller can be ignored when the circumferential structure of the volute is symmetry. However, the theoretical hypothesis is not valid for the centrifugal pump impeller. There are two following reasons: the first one is that the structure of the volute for a single centrifugal pump is unequal cross-section area, especially the volute tongue structure; the second one is the whirl motion of the impeller, which could induce n uneven flow and generate periodic fluid-induced force.

The fluid-induced force can be integrated by the transient pressure on each impeller wall in the unsteady calculation. The influence of eccentricity ratio ε, flow rate Q and rotation speed Ω on the fluid-induced force are analyzed. The 20 monitoring points on the outlet edge of the impeller with a certain interval angle 18°, shown in Fig. 4, are selected for better presentation and its corresponding static pressure values are calculated. P is the pressure in the pump which is monitored by the monitoring points. The pressure amplitude coefficient C_p and corresponding Root Mean Squared Error C_{pRMSE} can be calculated according to equation (1) and equation (2), respectively. C_{pRMSE} presents the uneven distribution of the impeller outlet pressure, the higher C_{pRMSE} means the greater pressure fluctuation.
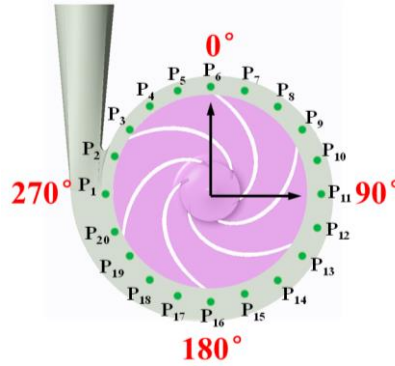
Fig. 4 Monitoring points around the outlet of impeller

$$C_p = \frac{P}{0.5\rho u_2^{\;2}} \tag{1}$$

$$C_{pRMSE} = \sqrt{\frac{1}{20}\sum_{i=1}^{n}(C_{pi} - \overline{C_p})^2} \tag{2}$$

In actual operation, a variety of flow conditions are always needed to meet the industrial requirements. Therefore, the transient fluid-induced forces under three flow conditions of $0.8Q_d$, $1.0Q_d$, $1.2Q_d$ are calculated, respectively. As shown in Figs. 5(a) ~ 5(c), on the whole, there are six peaks and troughs of fluid-induced force F_r under the three eccentricities, which is related to the rotor-stator interaction caused by the periodic sweeping of the six blades of impeller.
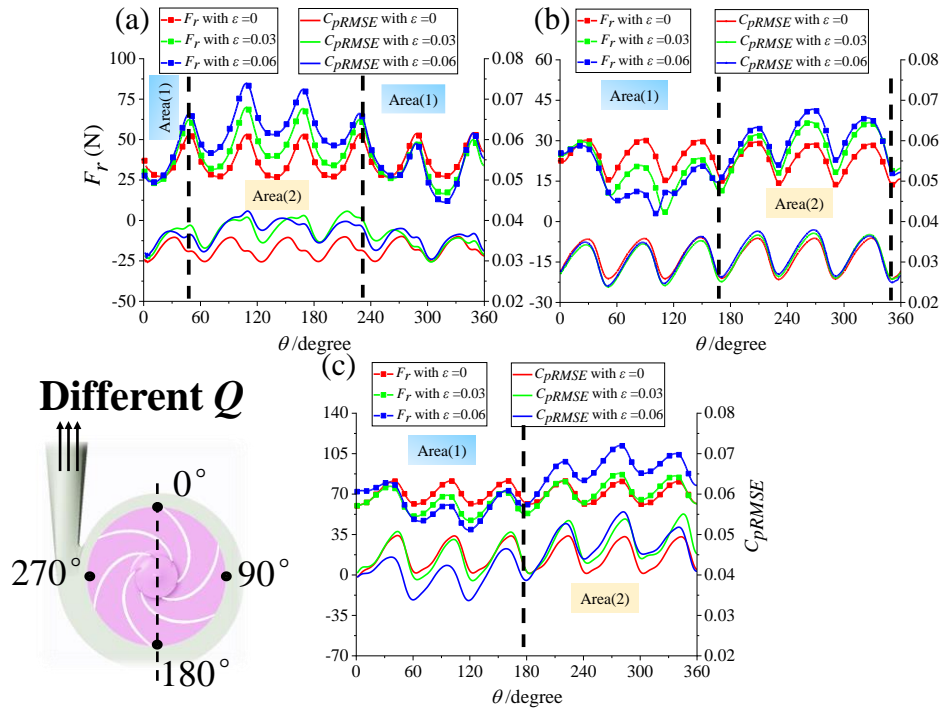
Fig. 5 Effects of different Q (a) $0.8Q_d$, (b) $1.0Q_d$ and (c) $1.2Q_d$ on the F_r and C_{pRMSE}

With the increase of the flow rate from $0.8Q_d$ to $1.2Q_d$, F_r presents obvious stratification phenomenon. Under the design flow rate, the fluctuation amplitude is minimum, which means that the change of the fluid-induced force is the lowest. At the same time, the average value of fluid-induced force F_{r-m} in periodic motion is calculated, the sequence of F_{r-m} for different flow rates is $F_{r-m(1.2Qd)} > F_{r-m(0.8Qd)} > F_{r-m(1.0Qd)}$ under the same impeller eccentricity. Trending curves of F_r and C_{pRMSE} show a positive correlation. The position distribution and interval distribution of the curves are consistent to a certain extent, which implies that the uneven distribution of the circumferential pressure of the impeller is an important source of the fluid-induced force.

It can also be seen that when the impeller is not eccentric, the extreme of the fluid-induced force under the three flow rates are stable. In addition, $F_{r(1.0Qd)}$ and $F_{r(1.2Qd)}$ in the range of $0°\sim180°$, which is far away from the volute tongue, are obviously smaller than those in the range of $180°\sim360°$ when eccentricity is considered. However, $F_{r(0.8Qd)}$ in Fig. 5(a) presents the opposite changing trend. Besides, with the increase of eccentricity, the fluctuation amplitude of F_r at non-design flow rate increases significantly and the corresponding distribution is more disordered compared with that at design flow rate. The similar conclusion is also suitable for C_{pRMSE}, the fluctuation amplitude of C_{pRMSE} at non-design flow rate is obviously larger than that at design flow rate when eccentricity is considered. The above calculated results imply that the non-design flow rate can significantly intensify the circumferential flow of the impeller and the fluid-induced force should not be regarded as a periodic force with same amplitude when the whirl motion effect is considered.

In order to study the influence of rotation speed on the fluid-induced force, the transient F_r at three different rotation speeds and different eccentricities is calculated. It can be seen from Fig. 6(a) ~ 6(c) that the number of peaks and troughs of F_r and C_{pRMSE} is also 6 due to the same number of blades. Under the same eccentricity, F_r curve has a similar shape and trend at different rotation speeds. The maximum value and range of F_r grows with the increase of the impeller eccentricity, and the average value of F_r in one cycle increases with the rise of rotation speed, which is $F_{r-m(1750rpm)} > F_{r-m(1450rpm)} > F_{r-m(1150rpm)}$.
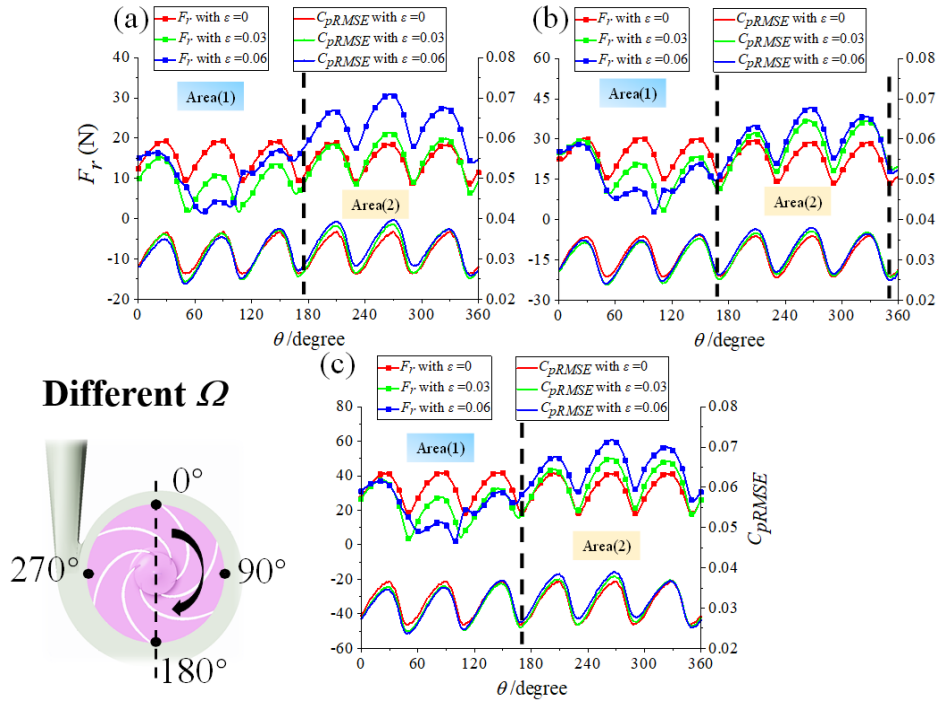
Fig. 6 Effects of different Ω (a) 1150rpm, (b) 1450rpm and (c) 1750rpm on the F_r and C_{pRMSE}

The above results show that although the internal flow of the centrifugal pump is similar after similarity transformation, the rotor-stator interaction intensity and turbulence intensity are still various at different rotation speeds, and they all increase with the rise of the rotation speed and the impeller eccentricity. The larger fluid-induced force and the oscillation amplitude mean a greater energy loss, which means that the design of the centrifugal pump parameters needs to coordinate various parameters to ensure higher efficiency and a more reasonable flow condition.

Meanwhile, as Fig. 6(a) ~ 6(c) show, the trend of C_{pRMSE} curve is positively correlated with the fluid-induced force curve, and the size distribution and interval distribution of the two curves under each working condition are very similar to a certain extent. In addition, the range and the average value of C_{pRMSE} under different eccentricities and rotation speeds are the same as the law of fluid-induced force F_r. The average value of C_{pRMSE} grows with the increase of rotation speed, which is the law of $C_{pRMSE-m(1750rpm)} > C_{pRMSE-m(1450rpm)} >$

$C_{pRMSE-m(1150rpm)}$. It shows that with the increase of the rotation speed, the dynamic and static interference between the impeller and the volute tongue is more intense, and the circumferential pressure distribution at the impeller outlet is more disordered at each moment, which means that the internal flow field distribution of the centrifugal pump is more uneven. The great consistency between the characteristics of C_{pRMSE} and fluid-induced force F_r shows that the dynamic and static interference between the impeller and the volute tongue is one of the important sources of the fluid-induced force.

5.2. Effects of ε, Q and Ω on pressure fluctuation

Through the above calculation and analysis, it is known that the impeller eccentricity has an obvious effect on the internal flow and unsteady characteristics of the centrifugal pump. Moreover, in order to better investigate the correlation mechanism between the unsteady flow characteristics and the fluid-induced force under the compound whirl motion, the pressure fluctuations considering the compound whirl effect at the monitoring points under different flow conditions and rotation speeds are further studied.

The monitoring point 2, which is closest to the volute tongue, and other monitoring points 3, 6, 12 and 17 are selected for the pressure fluctuation study. In the following figures, f_R and f_{BPF} mean the rotation frequency and blade passing frequency, respectively. In Fig. 7, it is seen that there are a lot of low frequency signals between 0 and f_{BPF}, and the shaft frequency increases significantly with the increase of the impeller eccentricity for $0.8Q_d$. That means the dynamic and static interference between the impeller and the volute tongue is more significant with the increase of the impeller eccentricity, which makes the internal flow of the centrifugal pump more disordered and increases the uneven distribution of the circumferential pressure in the impeller. Consequently, the macroscopic manifestation fluid-induced force would increase synchronously, which corresponds to the rule that F_r presents $F_{r-m\,(6\%)} > F_{r-m\,(3\%)} > F_{r-m\,(0\%)}$ in Fig. 5(a).
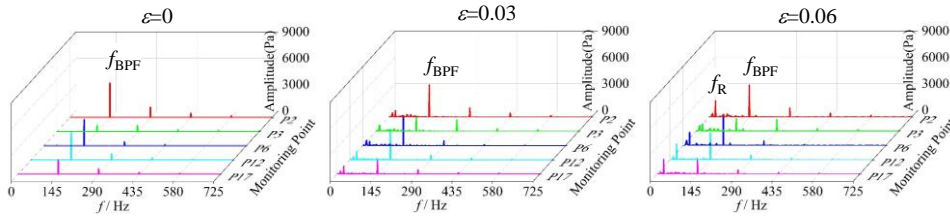
Fig. 7 Comparison of pressure spectrum of different monitoring points under $0.8Q_d$

As we known, the farther away from the monitoring point of the volute tongue, the smaller impact of the static and dynamic interference on it. In Figs. 8 and 9, f_{BPF} at the all monitoring points shows the same change of $f_{P2} > f_{P3} > f_{P6} > f_{P12} > f_{P17}$ in general. Therefore, the pressure fluctuation on the side near the volute tongue is larger, and the non-uniformity of the impeller circumferential pressure is more significant, which is also consistent with the calculated results in Fig. 5(b) and (c) that F_r shows a trend of $F_{r\,(6\%)} < F_{r\,(3\%)} < F_{r\,(0\%)}$ from $0°\sim180°$ and $F_{r\,(6\%)} > F_{r\,(3\%)} > F_{r\,(0\%)}$ from $180°\sim360°$.
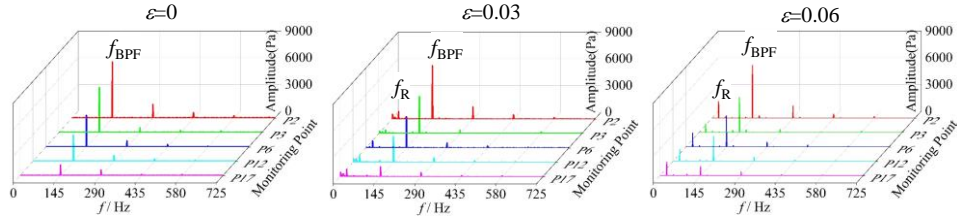
Fig. 8 Comparison of pressure spectrum of different monitoring points under $1.0Q_d$
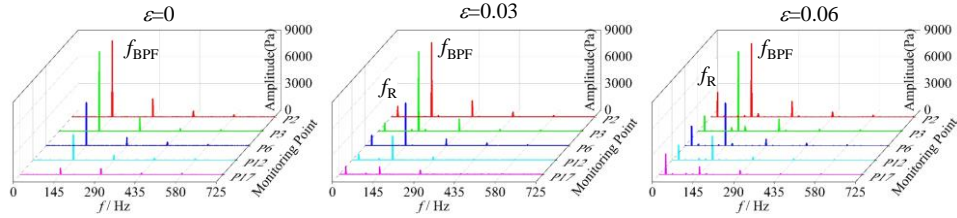
Fig. 9 Comparison of pressure spectrum of different monitoring points under $1.2Q_d$

Besides, f_R, f_{BPF} and $2f_{BPF}$ at the monitoring point P_2 are given more special attention and these data are extracted to research the mechanism, the corresponding amplitude are listed in Table 2. On the whole, when the impeller is eccentric, f_R increases significantly with the increase of the impeller eccentricity. At the same flow rate, with the increase of the impeller eccentricity, f_R enlarges and becomes more significant, f_{BPF} and $2f_{BPF}$ are reduced with the increase of the impeller eccentricity. In addition, f_R shows an inverse proportional relationship with the flow rate when the impeller is not eccentric. On the contrary, f_R, f_{BPF} and $2f_{BPF}$ increase with the flow rate when the compound whirl effect is considered.

Table 2 Amplitude of f_R, f_{BPF} and $2f_{BPF}$ of P_2 in different ε and Q

ε	Q/Q_d	f_R (Pa)	f_{BPF} (Pa)	$2f_{BPF}$ (Pa)
0	0.8	31.777	3971.309	1212.424
0	1.0	22.395	6324.310	1549.156
0	1.2	15.641	8575.916	2036.486
0.03	0.8	759.772	3612.386	1058.963
0.03	1.0	868.504	6024.788	1375.688
0.03	1.2	1223.527	8372.829	1831.697
0.06	0.8	1872.443	3654.332	1043.536
0.06	1.0	1893.877	5955.756	1367.366
0.06	1.2	2780.961	8271.600	1764.368

The effects of the compound whirl motion on the pressure fluctuation of the centrifugal pump at different rotation speeds are also calculated. It can be seen from Fig. 10 to Fig. 12 that the amplitude of the pressure fluctuation at the blade frequency of monitoring point P2 shows an upward trend with the increase of the impeller eccentricity, which corresponds to the rule that F_r presents $F_{r(6\%)} > F_{r(3\%)} > F_{r(0\%)}$ from 180°~360°in Fig. 6(a) to Fig. (c). Furthermore, compared with the calculated data for different rotation speeds, the amplitudes of the blade frequency and its octave frequency at each monitoring point become large with the rotation speed increase.
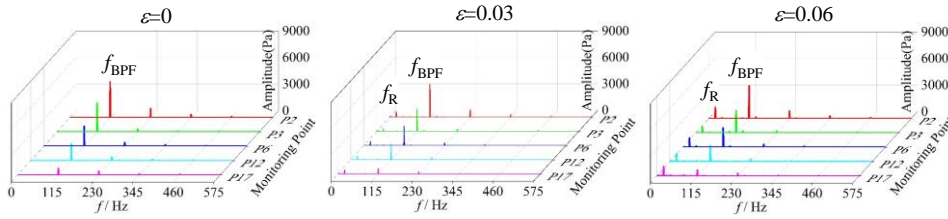
Fig. 10 Comparison of pressure spectrum of different monitoring points under 1150rpm
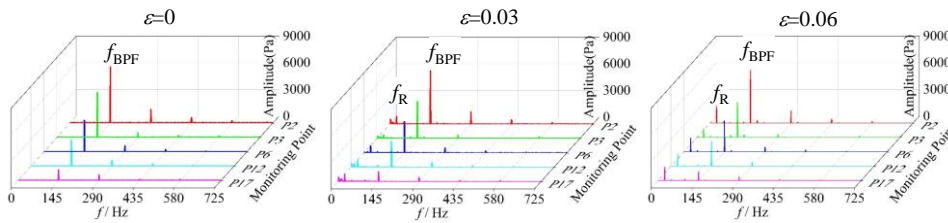
Fig. 11 Comparison of pressure spectrum of different monitoring points under 1450rpm
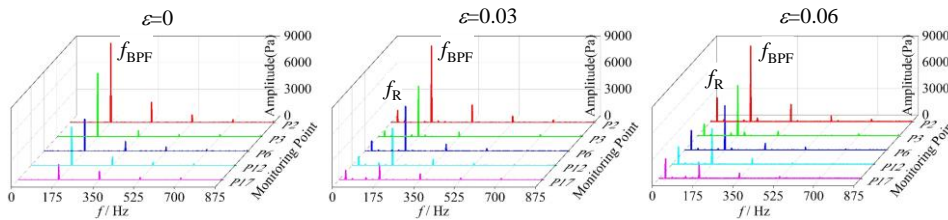
Fig. 12 Comparison of pressure spectrum of different monitoring points under 1750rpm

f_R, f_{BPF} and $2f_{BPF}$ at the monitoring point P_2 are also compared and analyzed in Table 3. At the same Ω, f_R increases significantly with the impeller eccentricity, and f_{BPF} and $2f_{BPF}$ with eccentricity are less than those without eccentricity. In addition, the change of f_R without the impeller eccentricity is limited, which means that f_R is not sensitive to the rotation speed if the compound whirl effect is not considered.

Table 3 Amplitude of f_R, f_{BPF} and $2f_{BPF}$ of P_2 in different ε and Ω

ε	Ω	f_R (Pa)	f_{BPF} (Pa)	$2f_{BPF}$ (Pa)
0	1150	28.2	4037.8	1011.9
0	1450	22.4	6324.3	1549.2
0	1750	25.5	9280.3	2303.7
0.03	1150	603.9	3722.8	853.6
0.03	1450	868.5	6024.8	1375.7
0.03	1750	1373.8	8652.7	1978.2
0.06	1150	1286.7	3730.9	861.6
0.06	1450	1893.9	5955.8	1367.4
0.06	1750	2747.7	8626.7	1970.1

f_{BPF} and $2f_{BPF}$ enlarge with the rotation speed increase when the impeller is eccentric, but it is almost the same after dimensionless in Table 4. Due to the similarity of flow, the

different impeller eccentricities and rotation speeds have little influence on the amplitude of f_{BPF} at the monitoring point, which can also explain the trend that the pressure coefficient C_{pRMSE} in Fig. 6 is almost the same for three different eccentricities. The results can help us to understand the correlation mechanism between the unsteady flow characteristics and the fluid-induced force of the centrifugal pump with the compound whirl motion more intuitively.

Table 4 Dimensionless amplitude of f_R, f_{BPF} and $2f_{BPF}$ of P_2 in different ε and Ω

ε	Ω	f_{BPF}	$2f_{BPF}$
0	1150	0.0330	0.0083
0	1450	0.0325	0.0080
0	1750	0.0327	0.0081
0.03	1150	0.0304	0.0070
0.03	1450	0.0310	0.0070
0.03	1750	0.0305	0.0070
0.06	1150	0.0304	0.0070
0.06	1450	0.0306	0.0070
0.06	1750	0.0304	0.0069

5.3. Effects of ε, Q and Ω on pressure distribution

Finally, the influence of the compound whirl motion for different flow rates and rotation speeds on the pressure distribution are researched. It can be seen from Fig. 13 that the turbulence in the centrifugal pump gradually develops fully with the change of the impeller eccentricity and the outlet pressure decreases with the flow rate increase.

Moreover, the pressure distribution gradient at the volute tongue presents the rule of $dp/dL_{(1.2Qd)} > dp/dL_{(0.8Qd)} > dp/dL_{(1.0Qd)}$ under the same impeller eccentricity, which is similar to the rule of $F_{r-m(1.2Qd)} > F_{r-m(0.8Qd)} > F_{r-m(1.0Qd)}$ in Fig. 5(a) ~ 5(c). The calculated results verify that the dynamic and static interference between the impeller and the volute tongue becomes more intense when the eccentricity of the impeller increases, which makes the flow condition of the centrifugal pump more disordered and increases the fluid-induced force near the volute tongue. It also shows that the dynamic and static interference between the impeller and the volute tongue is one of the important sources of the fluid exciting force.
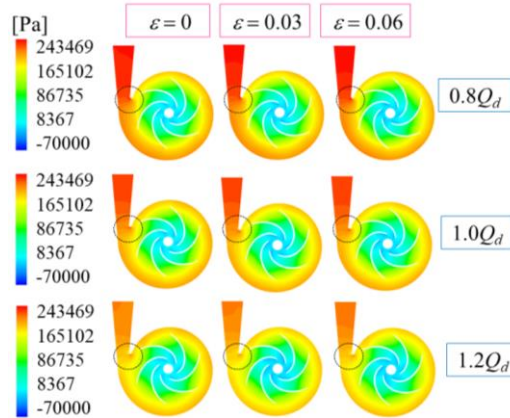
Fig. 13 Comparison of pressure distribution for different impeller eccentricities and flow rates
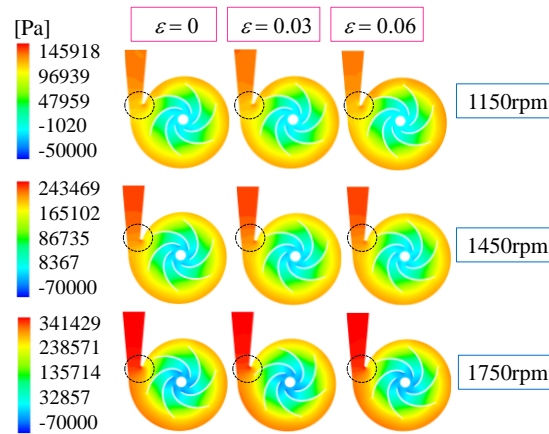
Fig. 14 Comparison of pressure distribution for different impeller eccentricities and rotation speeds

In Fig. 14, under the same impeller eccentricity, the uneven degree of pressure distribution around the impeller increases with the rise of rotation speed. The calculation results show that $dp/dL_{(1750rpm)} > dp/dL_{(1450rpm)} > dp/dL_{(1150rpm)}$, which verifies that the average value of the fluid exciting force in Fig.6(a) ~ 6(c) presents the distribution law of $F_{r-m(1750rpm)} > F_{r-m(1450rpm)} > F_{r-m(1150rpm)}$. In addition, at the same rotation speed, with the increase of the impeller eccentricity, the flow near the volute tongue is more turbulent. The flow near the volute tongue shows that $dp/dL_{(\varepsilon=0.06)} > dp/dL_{(\varepsilon=0.03)} > dp/dL_{(\varepsilon=0)}$, which is the same as the rule of $F_{r(\varepsilon=0.06)} > F_{r(\varepsilon=0.03)} > F_{r(\varepsilon=0)}$ in 180°~360°. This shows that the dynamic and static interference between the impeller and the volute tongue intensifies when the impeller eccentricity increases, which makes the uneven pressure distribution around the impeller more significant.

6. CONCLUSION

In this paper, a novel model considering the compound whirl motion is proposed to describe the actual motion of impeller and research the internal flow characteristics of centrifugal pump. The effects of eccentricity, flow rate and rotation speed on the fluid-induced force, pressure fluctuation and pressure distribution are mainly calculated. The mechanism correlation between the fluid-induced force and the internal flow characteristics are also analyzed and discussed. The main conclusions are as follows:

1. The proposed model considering the compound whirl effect can better describe the actual motion of the centrifugal pump compared with the present calculation model. The maximum errors of the head and the efficiency calculated by the novel model are 0.75% and 0.6%, respectively, while they are 2.29% and 1.75% calculated by the present model.

2. The fluid-induced force is sensitive to the impeller eccentricity. The fluid-induced force curve would change from smooth to steep when ε increase from 0 to 0.06. In addition, the fluid-induced force and the pressure coefficient of the circumferential pressure present a similar changing trend.

3. The dynamic and static interference between the impeller and the volute tongue becomes more evident with the increase of the impeller eccentricity, which makes the internal flow of the centrifugal pump more disordered and increases the uneven distribution of pressure around the impeller. Therefore, F_r near the volute tongue is larger than that away from the volute tongue.

4. Compared with the amplitudes of f_{BPF} and $2f_{BPF}$, the amplitude of f_R is more sensitive to the impeller eccentricity than flow rate and rotation speed. This is because the precession motion of the impeller, which has the same frequency with the rotation speed, increases the periodic dynamic and static interference between the impeller and volute tongue.

REFERENCES

1. Dong, L., Shang, H., Zhao, Y., Liu, H., Dai, C., Wang, Y., 2019, *Study on unstable characteristics of centrifugal pump under different cavitation stages*, Journal of Thermal Science, 28(4), pp. 608-620.
2. Li, W., Zhou, L., Shi, W. D., Ji, L., Yang, Y., Zhao, X., 2017, *PIV experiment of the unsteady flow field in mixed-flow pump under part loading condition*, Experimental Thermal and Fluid Science, 83, pp. 191-199.
3. Zhang, J., Li, G., Mao, J., Yuan, S., Qu, Y., Jia, J., 2020*, Numerical investigation of the effects of splitter blade deflection on the pressure pulsation in a low specific speed centrifugal pump,* Proceedings of the Institution of Mechanical Engineers, Part A: Journal of Power and Energy, 234(4), pp. 420-432.
4. Liang, D., Yuqi, Z., Cui, D., Yong, W., 2018, *Research on cavitation acoustic characteristics of centrifugal pump based on fluid-acoustic field coupling method*, Advances in Mechanical Engineering, 10(5), doi: 10.1177/1687814018773665.
5. Olimstad, G., Osvoll, M., Finstad, P H E., 2018, *Very Low Specific Speed Centrifugal Pump—Hydraulic Design and Physical Limitations*, Journal of Fluids Engineering, 140(7), 071403.
6. Chang, H., Li, W., Shi, W., Liu, J., 2018, *Effect of blade profile with different thickness distribution on the pressure characteristics of novel self-priming pump*, Journal of the Brazilian Society of Mechanical Sciences and Engineering, 40(11), 518.
7. Zhang, N., Liu, X., Gao, B., Xia, B., 2019, *DDES analysis of the unsteady wake flow and its evolution of a centrifugal pump*, Renewable Energy, 141, pp. 570-582.
8. Zhang, W., Yu, Z., Li, Y., Yang, J., Ye, Q., 2019, *Numerical analysis of pressure fluctuation in a multiphase rotodynamic pump with air–water two-phase flow*, Oil Gas Science and Technology, 74, 18.
9. Cao, W., Yao, L., Liu, B., Zhang, Y., 2017, *The influence of impeller eccentricity on centrifugal pump*, Advances in Mechanical Engineering, 9(9), doi: 10.1177/1687814017722496.
10. Liu, M., Tan, L., Cao, S., 2018, *Influence of geometry of inlet guide vanes on pressure fluctuations of a centrifugal pump*, Journal of Fluids Engineering, 140(9), 091204.
11. Bai, L., Zhou, L., Han, C., Zhu, Y., Shi, W., 2019, *Numerical study of pressure fluctuation and unsteady flow in a centrifugal pump*, Processes, 7(6), 354.
12. Zhang, N., Liu, X., Gao, B., Wang, X., Xia, B., 2019, *Effects of modifying the blade trailing edge profile on unsteady pressure pulsations and flow structures in a centrifugal pump*, International Journal of Heat and Fluid Flow, 75, pp. 227-238.
13. Yang, B., Li, B., Chen, H., Liu, Z., Xu, K., 2018, *Numerical investigation of the clocking effect between inducer and impeller on pressure pulsations in a liquid rocket engine oxygen turbopump*, Journal of Fluids Engineering, 141(7), 071109.
14. Tao, Y., Yuan, S., Liu, J., Zhang, F., 2019, *Influence of Cross-Sectional Flow Area of Annular Volute Casing on Transient Characteristics of Ceramic Centrifugal Pump*, Chinese Journal of Mechanical Engineering, 32(1), 4.
15. Chalghoum, I., Elaoud, S., Kanfoudi, H., Akrout, M., 2018, *The effects of the rotor-stator interaction on unsteady pressure pulsation and radial force in a centrifugal pump*, Journal of Hydrodynamics, 30(4), pp. 672-681.

16. Song, Y., Yu, Z., Shi, G., Liu, X., 2018, *Influence of impeller staggered arrangement on radial force and pressure fluctuation for a double-suction centrifugal pump*, Advances in Mechanical Engineering, 10(6), doi: 10.1177/1687814018781467.
17. Cui, B., Li, X., Rao, K., Jia, X., Nie, X., 2018, *Analysis of unsteady radial forces of multistage centrifugal pump with double volute*, Engineering Computations, 35(3), pp. 1500-1511.
18. Zou, Z., Wang, F., Yao, Z., Tao, R., Xiao, R., Li, H., 2016, *Impeller radial force evolution in a large double-suction centrifugal pump during startup at the shut-off condition*, Nuclear Engineering Design, 310, pp. 410-417.
19. Tao, R., Xiao, R., Liu, W., 2018, *Investigation of the flow characteristics in a main nuclear power plant pump with eccentric impeller*, Nuclear Engineering and Design, 327, pp. 70-81.
20. Hao, Y., Tan, L., Liu, Y., Xu, Y., Zhang, J., Zhu, B., 2017, *Energy performance and radial force of a mixed-flow pump with symmetrical and unsymmetrical tip clearances*, Energies, 10(1), 57.
21. Li, Y., Guo, D., Li, X., 2018, *Mitigation of radial exciting force of rotary lobe pump by gradually varied gap*, Engineering Applications of Computational Fluid Mechanics, 12(1), pp. 711-723.
22. Zhou, W., Zhao, Z., Wang, Y., Shi, J., Gan, B., Li, B., Qiu, N., 2021, *Research on leakage performance and dynamic characteristics of a novel labyrinth seal with staggered helical teeth structure*, Alexandria Engineering Journal, 60(3), pp. 3177-3187.
23. Jing, D., Hatami, M., 2020, *Peristaltic Carreau-Yasuda nanofluid flow and mixed heat transfer analysis in an asymmetric vertical and tapered wavy wall channel*, Reports in Mechanical Engineering, 1(1), pp. 128-140.
24. Zhai, L., Li, Y., Cui, B., Guo, J., Li, X., Zhu, Z., 2021, *Studies of cavitation characteristics of inducers with different blade numbers*, AIP Advances, 11(8), 085216.
25. Yao, Z., Wang, F., Zhang, Z., Xiao, R., He, C., 2015, *Numerical and experimental investigation on the radial force characteristic of a large double suction centrifugal pump in a real pumping station*, Fluids Engineering Division Summer Meeting, Seoul, 57212.
26. Tan, L., Shi, W., Zhang, D., Wang, C., Zhou, L., Mahmoud, E., 2018, *Numerical and experimental investigations on the hydrodynamic radial force of single-channel pumps*, Journal of Mechanical Science and Technology, 32(10), pp. 4571-4581.
27. Li, X., Gao, P., Zhu, Z., Li, Y., 2018, *Effect of the blade loading distribution on hydrodynamic performance of a centrifugal pump with cylindrical blades*, Journal of Mechanical Science and Technology, 32(3), pp. 1161-1170.
28. Barrio, R., Fernández, J., Blanco, E., Parrondo, J., 2011, *Estimation of radial load in centrifugal pumps using computational fluid dynamics*, European Journal of Mechanics - B/Fluids, 30(3), pp. 316-324.
29. Wang, K., Jing, Y., He, X., Liu, H., 2019, *Efficiency improvement and evaluation of a centrifugal pump with vaned diffuser*, Advances in Mechanical Engineering, 11(3), doi: 10.1177/1687814019825904.
30. Karaskiewicz, K., Szlaga, M., 2014, *Experimental and numerical investigation of radial forces acting on centrifugal pump impeller*, Archive of Mechanical Engineering, 61(3), pp. 445-454.
31. Zhou, W., Wang, Y., Li, C., Zhang, W., Wu, G., 2020, *Analysis of fluid-induced force of centrifugal pump impeller with compound whirl*, Alexandria Engineering Journal, 59(6), pp. 4247-4255.
32. Alemi, H., Nourbakhsh, A., Raisee, M., Farhad, A., 2015, *Development of new "multivolute casing" geometries for radial force reduction in centrifugal pumps*, Engineering Applications of Computational Fluid Mechanics, 9(1), pp. 1-11.
33. Jiang, W., Li, G., Liu, P. F., Fu, L., 2016, *Numerical investigation of influence of the clocking effect on the unsteady pressure fluctuations and radial forces in the centrifugal pump with vaned diffuser*, International Communications in Heat and Mass Transfer, 71, pp. 164-171.
34. Wang, L., Zhou, W., Wei, X., Zhai, L., Wu, G., 2016. *A coupling vibration model of multi-stage pump rotor system based on FEM*, Mechanika, 22(1), pp. 31-37.
35. Ye, X., Wang, J., Zhang, D., Hu, J., Feng, Y., 2014, *The dynamic characteristic analysis of the water lubricated bearing-rotor system in seawater desalination pump*, Advances in Mechanical Engineering, 6, doi: 10.1155/2014/356578.
36. Zhou, W., Qiu, N., Wang, L., Gao, B., Liu, D., 2018, *Dynamic analysis of a planar multi-stage centrifugal pump rotor system based on a novel coupled model*, Journal of Sound and Vibration, 434, pp. 237-260.
37. Li, W., Shi, W., Jiang, X., Hu, J., Ye, X., Tian, H., 2015, *Research on the liquid film force of water lubricated bearing in desalination multistage pumps and its coupled dynamics with rotor*, Journal of Coastal Research, 73, pp. 453-459.
38. Li, W., Ji, L., Shi, W., Wang, Y., Zhou, L., Jiang, X., 2018, *Vibration of shaft system in the mixed-flow pump induced by the rotor-stator interaction under partial load conditions*, Shock and Vibration, 2018, 2059784.
39. Zhou, W., Cao, Y., Zhang, N., Gao, B., Qiu, N., Zhang, W., 2019, *A novel axial vibration model of multistage pump rotor system with dynamic force of balance disc*, Journal of Vibration Engineering Technologies, 8(5), pp. 673-683.

40. Wang, K., Luo, G., Li, Y., Xia, R., Liu, H., 2020, *Multi-condition optimization and experimental verification of impeller for a marine centrifugal pump*, International Journal of Naval Architecture and Ocean Engineering, 12, pp. 71-84.
41. Lin, P., Li, Y., Xu, W., Chen, H., Zhu, Z., 2020, *Numerical Study on the Influence of Inlet Guide Vanes on the Internal Flow Characteristics of Centrifugal Pump*, Processes, 8(1), 122.
42. Zhang, N., 2016, *Excitation characteristics induced by unsteady flow within a centrifugal pump*, PhD Thesis, Jiangsu University, China. (in Chinese)